Numerical Study of Opposed-Flow Flame Spread over Charring Solids

Won Chan Park[†], Arvind Atreya[†] and Howard R. Baum[‡]

Numerical calculations were performed on thermal decomposition of charring solids undergoing opposed-flow flame spread and the results are compared with analytical models developed by Baum and Atreya [1-2]. The objective was to understand the effect of finite rate kinetics on the temperature and pressure inside the solid. The analytical solution, while exact, assumes infinite kinetics, i.e. abrupt decomposition at a known pyrolysis temperature. The numerical results using finite and infinite rate kinetics showed good agreements with the analytical model in terms of char depth and temperature distribution. For the solution of the pressure equation, numerical results showed good agreements with analytical gas transport model from surface to char/virgin solid interface. However, the numerical result using finite kinetics implies that pressurized region in real situation is larger than that of infinite kinetics assumption. Numerical analysis using infinite kinetics showed pressure fluctuation due to lack of the information of the interface shape inside a cell.

1. Introduction

The prediction of fuel gas generation from a charring solid undergoing opposed-flow flame spread is complicated because the gas is generated in the pyrolysis zone under the char layer. Fig. 1 shows the schematic diagram of the physical problem. The heat required for thermal decomposition must be provided by conduction through the char layer from the surface which is heated by the flame. The fuel gas is pushed from the pyrolysis zone to the surface through void spaces in the char layer by the pressure gradient generated inside the charring solid. In the real situation, fuel gas generation and ejection is related to many complex chemical and physical aspects such as multiple finite reaction kinetics, change of material properties with temperature and degree of pyrolysis, anisotropic material properties, and convective cooling of the char layer due to gas flow. Recently, an analytical model for opposed flow flame spread over a charring solid is developed by Atreya and Baum [1] based on simplified assumptions. Their model uses infinite rate kinetics where the virgin material pyrolyzes to char abruptly at a specified pyrolysis temperature. The model solves for the char layer thickness and the temperature profiles in both the char and the virgin solid. The model assumes that gases are transported from the pyrolysis zone to the surface instantly after generation without any effect on the char layer. Pressure distribution inside the char layer and the effect on the temperature of the char layer were not considered. Subsequently, Baum et al [2] developed an analytical model for transport of gases in charring solid. This model solves for the gas pressure distribution based on char layer profile and temperature distribution obtained earlier by Atreya and Baum [1]. The purpose of this study is to numerically investigate the charring behavior during flame spread and examine the assumptions made in the analytical model. Until now, numerical analysis has been performed on conditions similar to the analytical model. In the future, realistic phenomena such as multiple step finite rate pyrolysis kinetics, temperature dependent material properties, etc. will be added to understand their effect on flame spread.

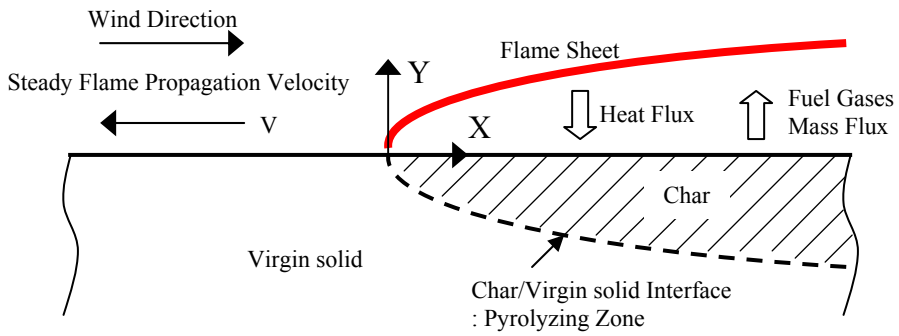

Fig. 1. Schematic of the physical problem : steady propagation of an opposed-flow diffusion flame on the surface of a charring solid

2. Energy Equation

2.1 Analytical Model

Atreya and Baum [1] developed an analytical model for energy equation in the char layer and virgin solid using parabolic coordinates defined by the relation:

$$\tau + i\omega = \sqrt{\frac{2V}{\alpha_v}(x + iy)} \tag{1}$$

[†] Department of Mechanical Engineering, University of Michigan, Ann Arbor, MI 48109
[‡] Building and Fire Research Laboratory, National Institute of Standard and Technology, Gaithersburg, MD 20899

Here V and α_v are flame spread speed ($V = 0.001 m/s$) and the thermal diffusivity of the virgin solid. In the model, temperature is assumed as a function only of ω. For boundary conditions, no heat exchange is assumed between the atmosphere and the solid upstream of the flame inception point ($x < 0$, $y = 0$) and constant surface temperature is assumed in the downstream region ($x > 0$, $y = 0$). At the interface, ω is defined as c which is obtained by solving eq. (4) below. Temperature distributions in char and virgin solid are described in eqs. (2) & (3). Material properties used in this numerical study are from Di Blasi [3], where the reaction heat liberated at the pyrolysis temperature T_p is: $Q = 497302.6$ J/kg ; $T_p = 598.16K$; ambient temperature $T_\infty = 298.16K$; surface temperature $T_s = 1298.16K$; specific heat capacities of virgin solid and char $C_v = 1400 J/kg\,K$, $C_c = 1100 J/kg\,K$; thermal conductivities $\lambda_v = 0.209 W/m\ K$, $\lambda_c = 0.071 W/m\,K$; the densities of final char and the original virgin solid $\rho_{c0} = 140 kg/m^3$, $\rho_{v0} = 700 kg/m^3$. The value of 'c' based on these properties is found to be: $c = 0.4619$.

$$T_v(\omega) = T_p F(\omega) , \qquad F(\omega) = \frac{T_\infty}{T_p} + \left(1 - \frac{T_\infty}{T_p}\right) \frac{erfc\left(\frac{\omega}{\sqrt{2}}\right)}{erfc\left(\frac{c}{\sqrt{2}}\right)} \tag{2}$$

$$T_c(\omega^*) = T_p G(\omega^*), \qquad G(\omega) = \frac{T_s}{T_p} - \left(\frac{T_s}{T_p} - 1\right) \frac{erfc\left(\frac{\omega^*}{\sqrt{2}}\right)}{erfc\left(\frac{c^*}{\sqrt{2}}\right)} \qquad \text{where } c^* = \sqrt{\frac{\alpha_v}{\alpha_c}} c , \quad \omega^* = \sqrt{\frac{\alpha_v}{\alpha_c}} \omega \tag{3}$$

$$\left\{ \frac{\lambda_c}{\lambda_v} \frac{T_s - T_p}{T_p - T_\infty} \sqrt{\frac{\alpha_v}{\alpha_c}} \right\} \left\{ \frac{\exp\left(-\frac{c^2}{2} \frac{\alpha_v}{\alpha_c}\right)}{erf\left(\sqrt{\frac{\alpha_v}{2\alpha_c}} c\right)} \right\} - \frac{\exp\left(-\frac{c^2}{2}\right)}{erfc\left(\frac{c}{\sqrt{2}}\right)} = \frac{Q}{C_{pv}(T_p - T_\infty)} \sqrt{\frac{\pi}{2}} c \tag{4}$$

2.2 Numerical Analysis

Numerical analysis has been conducted for the same conditions as the analytical model. Energy conservation equation in the charring solid is shown below; eq. (5). $\vec{V} = V\hat{i}$ is the virgin solid feeding velocity which has the same magnitude and opposite direction as the flame spread rate. Since the thermal effect of the gas is neglected, energy equation only includes the solid phase components; $\rho C = \rho_v C_v + \rho_c C_c$. Since the physical problem is steady state, the unsteady term on the left hand side vanishes as time step proceeds and the steady state solution is obtained.

$$\rho C \frac{\partial T}{\partial t} + \rho C \vec{V} \bullet \vec{\nabla} T = \vec{\nabla} \bullet \left(\lambda \vec{\nabla} T\right) + S_v Q \tag{5}$$

Mass conservation of the solid phase components is determined by the convective mass flux due to the feeding velocity and mass generation due to pyrolysis at the interface; eq. (6). Here, ρ_c and ρ_v represent the instantaneous densities of char and virgin solid in a cell and S_v is the mass pyrolysis rate per unit volume of the virgin solid.

$$\frac{\partial \rho_v}{\partial t} + \vec{V} \bullet \vec{\nabla} \rho_v = S_v \tag{6}$$

Physical domain chosen for the numerical calculations is: $-0.1m \le x \le 0.1m$, $-0.01m \le y \le 0m$ and 160×160 mesh was used.

Infinite Reaction Kinetics

Since the analytical model is based on infinite reaction kinetics and treats pyrolysis as discontinuous step function, numerical analysis has been performed with the same conditions. For the cell which has the interface inside, the temperature is set to T_P and the pyrolysis rate is determined by energy balance resulting from conduction heat transfer, convection due to the feeding velocity and the heat of pyrolysis. For the cells inside the char layer, the entire amount of virgin solid influx from the upstream cell is pyrolyzed.

For interface cells ($\rho_v > 0$, $\rho_c > 0$)

$$T = T_P , \qquad S_v = \frac{\rho C \vec{V} \bullet \vec{\nabla} T - \vec{\nabla} \bullet \left(\lambda \vec{\nabla} T\right)}{Q} \tag{7}$$

For the cells inside the char layer ($\rho_v = 0$, $\rho_c = \rho_{c0}$)

$$S_v = \vec{V} \bullet \vec{\nabla} \rho_v \tag{8}$$

Finite Reaction Kinetics

Using infinite reaction kinetics causes numerical difficulties due to incorrect interface shape inside the cell. Since the interface cell does not have the information of this shape, the interface was regarded as a horizontal line based on densities of the solid components. To overcome this difficulty, finite reaction kinetics which is an Arrhenius function of temperature has been implemented in the numerical analysis. The pre-exponential constant k and the activation energy E_a used in this study are significantly higher than realistic values. These values are arbitrarily chosen to simulate infinite rate kinetics and obtain the best match with the analytical model.

$$S_v = -\rho_v k e^{-\frac{E_a}{RT}} \tag{9}$$

Here, $k = 1.0 \times 10^{24}$, $E_a = 288{,}000 J/mol$, universal gas constant $R = 8.314 J/molK$.

2.3 Energy Equation Results

Calculated char/virgin solid interfaces are shown in Fig. 2. For the analytical model, char/virgin solid interface is determined by 'c' and expressed by:

$$\left(\frac{Vy}{\alpha_v}\right)^2 = c^2 + 2c\left(\frac{Vx}{\alpha_v}\right)^2 \tag{10}$$

Both numerical results with infinite reaction kinetics and finite reaction kinetics show excellent agreement with the analytical model. Since an obvious interface does not exit in the case of finite reaction kinetics, 50% pyrolyzed position is regarded as the interface. However, 5% and 95% pyrolyzed positions are also plotted to show the width of the pyrolysis zone. Even though unrealistically large values of the pre-exponential factor and the activation energy were used, the pyrolysis zone width is considerable. The finite kinetics case does not have a distinct char/virgin solid interface but shows a continuous change of char/virgin solid composition. Nonetheless, if real pyrolysis reactions with finite kinetics can be simplified by infinite kinetics with proper values of the pyrolysis temperature and reaction heat, analytical model would be very useful in fire research because it does not require huge computation time and resources as numerical computation does. Temperature distribution in the charring solid and char/virgin solid interface of the numerical results of infinite rate kinetics and finite rate kinetics are shown in Fig. 3 and 4. The temperature distribution shows nearly identical profiles between the results of both infinite and finite kinetics. The results of this study imply that the analytical model would predict char depth and temperature field in real situation quite accurately as can be seen from Fig. 3 and 4. However, proper choice of pyrolysis temperature and heat of reaction is required for accurate prediction.

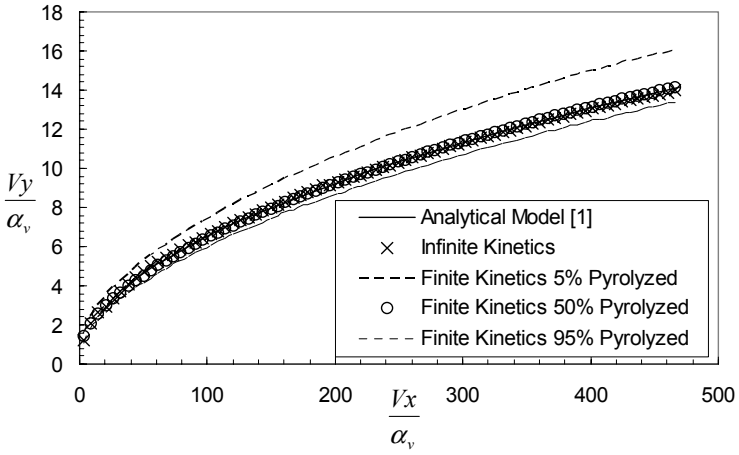

Fig. 2 Char layer thickness in dimensionless length: (1) Analytical model [1], (2) Numerical analysis result using infinite reaction kinetics and (3) Numerical analysis result using finite reaction kinetics (5%, 50% and 95% pyrolyzed)

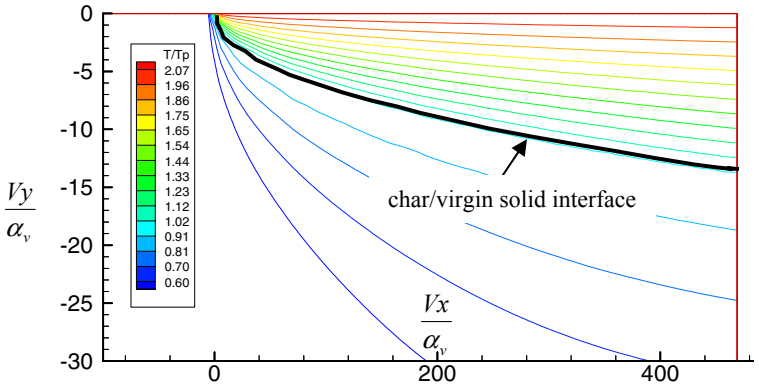

Fig. 3 Temperature distribution and char/virgin solid interface of numerical results using infinite reaction kinetics

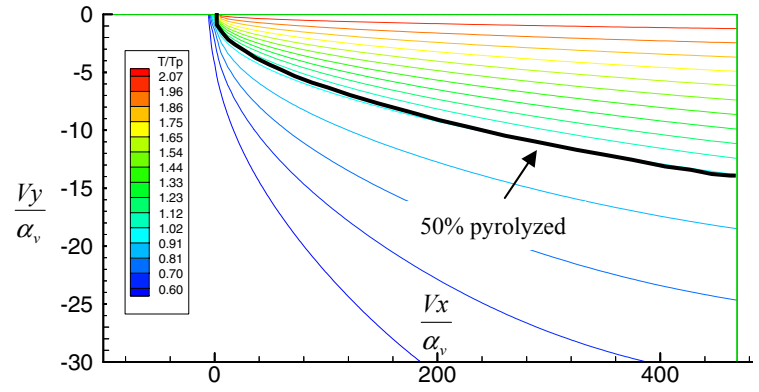

Fig. 4 Temperature distribution and char/virgin solid interface of numerical results using finite reaction kinetics

3. Pressure Equation

3.1 Analytical Model

An analytical model for gas transport in charring solids has been developed by Baum et. al [2] based on their precious work [1]. This gas transport model makes the following assumptions for the gas flow and boundary conditions:

(1) The gas flow through void spaces in char follows Darcy's law: $\bar{u} = -\dfrac{B}{\mu(T)}\vec{\nabla}P$,

(2) Surface pressure in the downstream zone ($x > 0$, $y = 0$) is ambient pressure,

(3) The virgin solid is impermeable. Thus, the gas transport equation is solved only in the char layer and pressure gradient normal to the char/virgin solid interface is zero.

The final pressure equation is:
$$\beta\omega^* \frac{d}{d\omega}\left(\frac{P(\omega^*)}{G(\omega^*)}\right)+\left(\frac{P(\omega^*)}{\left[G(\omega^*)\right]^{n+1}}\frac{dP(\omega^*)}{d\omega^*}\right)=0 \tag{11}$$

Where, the non-dimensional pressure $p(\omega^*)= p_s P(\omega^*)$, surface pressure $P_s = 101300Pa$, gas viscosity is a function of temperature $\mu(\omega^*)= \mu_p\left[G(\omega^*)\right]^n$, viscosity at pyrolysis temperature $\mu_p = 3.0\times10^{-5} kg/ms$, transport parameter $\beta = \dfrac{\varepsilon\alpha_c\mu_p}{P_s B}$, permeability of char $B = 1.0\times10^{-13} m^2$, and porosity $\varepsilon = 0.8$.

Gas transport boundary conditions are: $P(\omega^*)\dfrac{dP}{d\omega^*} = c^*\dfrac{\rho_v T_p}{\rho_s T_s}\beta \quad (\omega^* = c^*); \qquad P(0)=1 \quad (\omega^* = 0)$ (12)

3.2 Numerical Analysis

The mass conservation equation for gas in the char is described by eq. (13) below. The gas flow through voids in the char is assumed to follow Darcy's law as in the analytical model. Gas in the void spaces is assumed as an ideal gas [eq. (14)]; therefore, the final pressure equation is derived from eqs. (13) and (14)

Mass conservation equation for gas:
$$\frac{\partial\varepsilon\rho_g}{\partial t} = \vec{\nabla}\bullet\left(\rho_g\frac{B}{\mu}\vec{\nabla}p\right)-\vec{\nabla}\bullet\left(\varepsilon\rho_g\vec{V}\right)-\left(1-\frac{\rho_{c0}}{\rho_{v0}}\right)S_v \tag{13}$$

Equation of state:
$$\varepsilon\rho_g = \frac{\varepsilon M_g}{RT}p_g \tag{14}$$

Pressure equation:
$$\frac{\varepsilon}{T}\frac{\partial p}{\partial t}-\frac{\varepsilon p}{T^2}\frac{\partial T}{\partial t}+\frac{p}{T}\frac{\partial\varepsilon}{\partial t}=\frac{R}{M_g}\left(\vec{\nabla}\bullet\left(\rho_g\frac{B}{\mu}\vec{\nabla}p\right)-\vec{\nabla}\bullet\left(\varepsilon\rho_g\vec{V}\right)-\left(1-\frac{\rho_{c0}}{\rho_{v0}}\right)S_v\right) \tag{15}$$

Here, the gas molecular weight is $M_g = 0.018 kg/mol$. As unsteady terms vanish, steady pressure field is obtained.

In the analytical model, the solution of the energy equation is used for determining the pressure. In this numerical study, pressure has been determined in three different ways: (1) analytical model result for temperature obtained from reference [1], (2) numerical calculations with infinite reaction kinetics, as shown in figure 3, and (3) numerical calculations with finite reaction kinetics, as shown in figure 4. In cases (1) and (2), an obvious char/virgin solid interface exits. However, in the case (3), there is no distinct interface due to a continuous pyrolysis zone. For this reason, the definition of the char layer or the pressure analysis domain has to be determined. In this study, domain for $\rho_c \geq 1.0 kg/m^3$ is regarded as char layer which is larger than that of (1) and (2).

3.3 Results of Pressure Calculations

As mentioned previously, three cases of numerical analysis for the pressure field have been conducted and compared with the analytical model [2]. Pressure distributions with regards to ω^* are plotted in Fig. 5 from surface to the char/virgin solid interface $(0 < \omega^* < 0.3)$. Pressure contours inside char are plotted in Figures 6, 7 and 8. We note that while the contours in figure 6 are smooth as expected, those in figure 7 fluctuate. The condition improves in figure 8 because of smooth transition from wood to char. Thus, the pressure plot in figure 5 was obtained by averaging over 25% ~ 75% of total x-directional length of the char layer. The pressure calculations based on the analytical temperature field is closet to the analytical pressure

solution as expected. Considerable pressure fluctuation is observed in infinite kinetics case (figure 7). This pressure fluctuation is caused by the fluctuations in the gas generation rate which is clearly shown Fig. 9. In other cases, gas generation rate shows a gradually decaying pattern with *'x'*. The gas generation rate is obtained differently for each case. In case of infinite kinetics, the gas generation rate is calculated by energy balance or the amount of virgin solid influx. The assumption of horizontal interface in the cell causes variations in the gas generation rate, although the overall average gas generation rate matches with the other cases. For finite kinetics, the gas generation rate is calculated by a continuous function of temperature. Therefore it shows gradually decaying pattern. For analytical temperature field, the gas generation rate is obtained by the virgin solid density difference of influx and efflux based on the known interface shape. Hence the results are very smooth.

Since obvious char/virgin solid interface does not exit for finite kinetics, pressure computation domain is not obvious. In this study, pressure is computed for the domain where char density is greater than $1.0 kg/m^3$. Consequently, pressure computation domain for finite kinetics case is larger than the other cases whose domain is defined by a distinct interface. Fig. 8 shows a larger pressure distribution domain. This is closer to the real case where the permeability of the virgin solid does not go to zero at the interface. Yet, the agreement between the models is remarkable. It is also noted that the permeability of the virgin solid is thousands times smaller than that of char; thus, the permeability in char/virgin solid mixed cell should be adjusted by the degree of pyrolysis. Since all analysis performed in this study used constant permeability of char, the pressure results are expected to be lower than the real situation. The effect of these factors will be investigated in the future.

4. Conclusions and Future Work

A numerical study was performed on thermal degradation of charring solid undergoing opposed flow flame spread and compared with analytical models of references [1] & [2]. For the solution of the energy equation, both numerical results using finite and infinite kinetics showed good agreements with the analytical model in terms of char depth and temperature distribution. For the solution of the pressure equation, numerical results showed good agreements with analytical gas transport model from surface to char/virgin solid interface. However, the numerical result of finite kinetics showed that considerable area below the interface is pressurized. The effects of several factors such as coupling of energy and pressure equation, permeability, convection cooling of char and multiple finite pyrolysis kinetics will be numerically investigated and used to evaluate the performance of the analytical model.

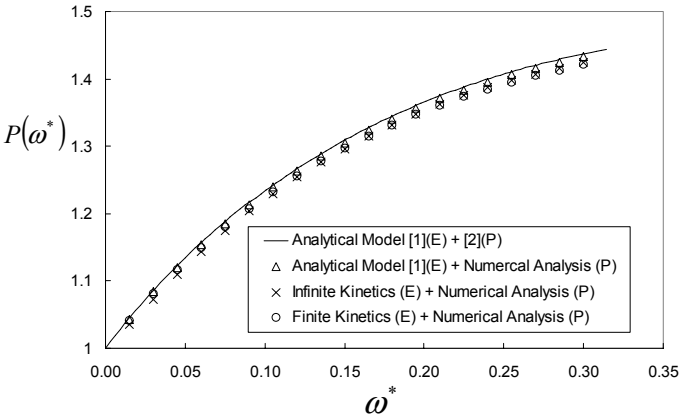

Fig. 5 Pressure distribution in the char layer: pressure distribution on ω^* is averaged value over 25% ~ 75% of total char layer length. (1) Analytical models for both energy and pressure, (2) Analytical model for energy + numerical analysis for pressure, (3) Numerical analysis for both energy and pressure, finite reaction kinetics for energy and (4) Numerical analysis for both energy and pressure, finite reaction kinetics for energy; (E) and (P) mean energy equation and pressure equation.

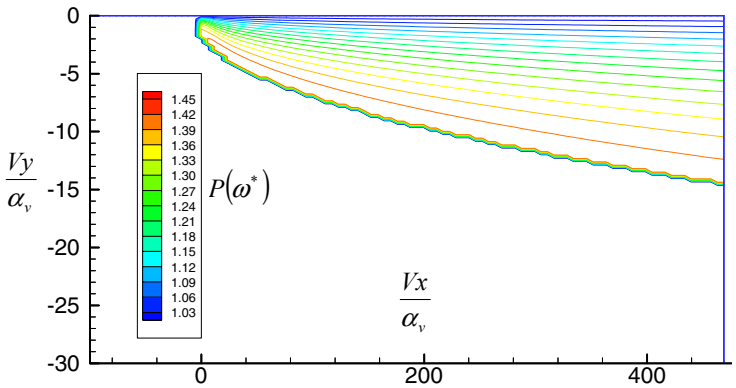

Fig. 6 Pressure distribution of numerical results based on analytical model for energy equation

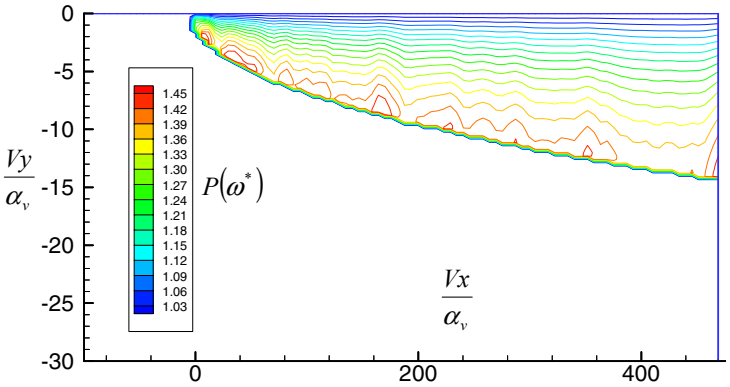

Fig. 7 Pressure distribution of numerical results based on infinite reaction kinetics

Nomenclature

B	permeability of char $[m^2]$
C	specific heat at constant pressure $[J/kg\,K]$
c	charring constant defining the location of char/virgin solid interface
E_a	activation energy $[J/mol]$
F, G	non-dimensional temperature
k	pre-exponential constant
M	molecular weight $[kg/mol]$
P	non-dimensional pressure
Q	heat liberated or absorbed at the interface per unit mass of virgin solid $[J/kg]$
R	universal gas constant $[J/molK]$
S	mass pyrolysis rate per unit volume $[kg/m^3\,\mathrm{s}]$
T	temperature $[K]$
t	time $[s]$
V	flame spread speed $[m/s]$
x, y	Cartesian coordinates $[m]$

Greek Symbols

α	thermal diffusivity $[m^2/s]$
β	transport parameter
ε	porosity
λ	thermal conductivity $[W/m\,K]$
μ	dynamic viscosity of gas $[kg/m\,s]$
ρ	density $[kg/m^3]$
τ, ω	parabolic coordinates

Subscripts

c	char
$c0$	final state of char
v	virgin solid
$v0$	original state of virgin solid
g	gas
p	pyrolysis
s	surface
∞	ambient condition

References

[1] Atreya, A. and Baum, H.R., "A Model of Opposed-Flow Flame Spread Over Charring Materials", Proc. Combustion Institute, Vol. 29, pp. 227-236, (2002)

[2] Howard R. Baum and Arvind Atreya, "Transport of Gases in Charring Solids", Proc. Joint Meeting of U.S. section of the Combustion Institute, (2005)

[3]C. Di Blasi, "Modeling the fast pyrolysis of cellulosic particles in the fluid-bed reactors", Chemical Engineering Science,55, 5999-6013, (2000)

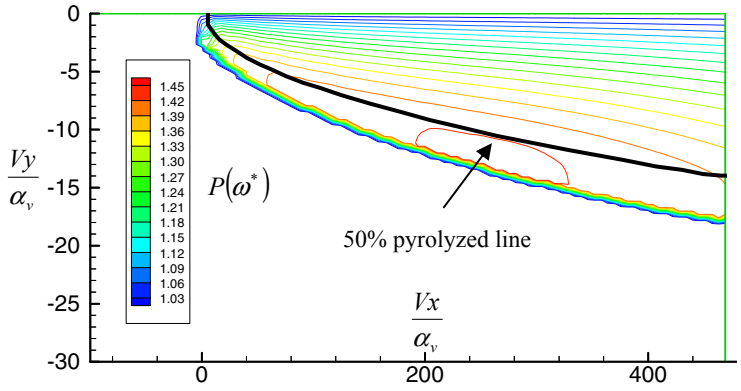

Fig. 8 Pressure distribution of numerical results based on finite reaction kinetics

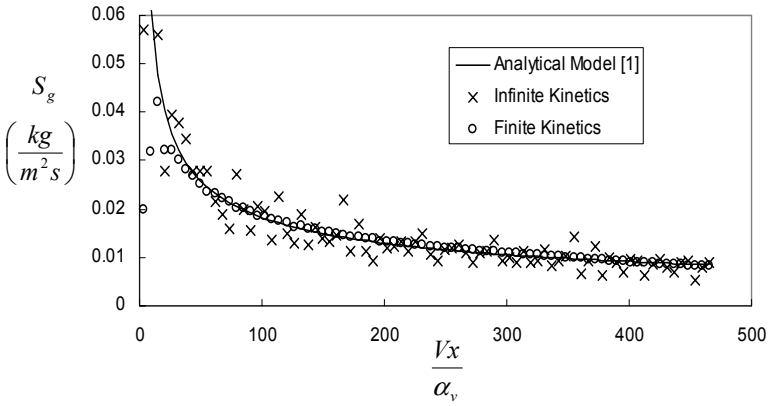

Fig. 9 Gas generation rate: (1) Analytical Model [1], (2) Numerical analysis using infinite reaction kinetics and (3) Numerical analysis using finite reaction kinetics